Role of the Special Pair in the Charge-Separating Event in Photosynthesis

Hidekane Ozeki,[a] Akihiro Nomoto,[a] Kazuya Ogawa,[a] Yoshiaki Kobuke,*[a] Masataka Murakami,[b] Kou Hosoda,[b] Masana Ohtani,[b] Satoru Nakashima,[b] Hiroshi Miyasaka,[b] and Tadashi Okada[b]

Abstract: We synthesized special-pair/electron-acceptor systems consisting of a complementary slipped cofacial dimer of imidazolyl-substituted zinc porphyrin, bearing pyromellitdiimide as the electron acceptor. In the case of the dimer, the first and second oxidation potentials were split into a total of four peaks in the differential pulse voltammetry measurement. Furthermore, the shift values of the first oxidation potentials obtained by changing the solvent polarity for the dimer were almost half of those observed for the monomer. These results indicate that the radical cation is delocalized over the whole π system of the dimer. Time-resolved transient absorption measurements revealed that, relative to the corresponding monomer, the dimer accelerated the charge separation rate, but decelerated the charge recombination rate. The smaller reorganization energy of the slipped cofacial dimer relative to that of the monomeric system demonstrates the significance of the special-pair arrangement for efficient charge separation in photosynthesis.

Keywords: electron transfer · photochemistry · photosynthesis · porphyrinoids · self-assembly

Introduction

The primary charge-separating event in the bacterial photosynthetic reaction center occurs at the "special pair", in which a bacteriochlorophyll dimer ejects an electron in response to optical excitation, thereby generating the radical cation. This is the first step in the photoinduced redox process and is followed by transmembrane electron transfer to convert light into chemical energy.[1] The structures of the special pair in photosynthetic reaction centers have been determined by using X-ray crystallography to be two bacteriochlorophyll planes held together in a slipped cofacial orientation at a close distance of 3.1–3.6 Å.[2] Despite numerous studies of models of the reaction centers of photosynthetic systems,[3,4] incorporation of a special pair into these models has been limited to only Gable-type porphyrin dimers,[5] in which two porphyrins are bridged by an *o*-phenylene linker. The dimer that is composed of two monomeric zinc porphyrin moieties, which bear a pyromellitdiimide (1,2,4,5-benzenetetracarboxydiimide, PI) group as an electron acceptor, was synthesized to achieve the long-lived charge-separated state; the lifetime of this state depends on solvent polarity[5a]. The structural model introduced by us[6] mimicks the geometry of natural systems, as it includes a complementary imidazolyl-to-zinc coordination, and enables two chromophoric π orbitals to interact strongly in a slipped, cofacial arrangement. The zinc complex of the imidazolyl porphyrin exists quantitatively as a slipped cofacial dimer, similar to compound **1** (see Formula), with an extremely large self-association constant of the order of $10^{11}\,\text{M}^{-1}$ in nonpolar media, such as chloroform, by complementary coordination. Because the zinc ion in a porphyrin ring can accept only one axial coordination, no further propagation can occur. The complementary dimer shows a split of the Soret band with splitting energy of $\sim 1035\,\text{cm}^{-1}$, due to strong excitation coupling between the two porphyrins. On the other hand, even such a stable dimer can be dissociated by the addition of a competing ligand, such as MeOH, imidazole, or pyridine, to a monomer with a convergence into the single Soret band. The ability of this complementary coordination to represent the special pair was demonstrated, with some structural modifications,[7,8] but the functional role of the artificial special pair has remained unsolved. The spectrum of the one-

[a] Dr. H. Ozeki, Dr. A. Nomoto, Dr. K. Ogawa, Prof. Y. Kobuke
Graduate School of Materials Science
Nara Institute of Science and Technology
8916-5 Takayama, Ikoma, Nara 630-0101 (Japan)
Fax: (+81) 743-72-6119
E-mail: kobuke@ms.naist.jp

[b] Dr. M. Murakami, K. Hosoda, M. Ohtani, Dr. S. Nakashima, Prof. H. Miyasaka, Prof. T. Okada
Department of Chemistry
Graduate School of Engineering Science, Osaka University
Toyonaka, 560-8531 (Japan)

Supporting information for this article is available on the WWW under http://www.chemeurj.org/ or from the author.

 DOI: 10.1002/chem.200400624

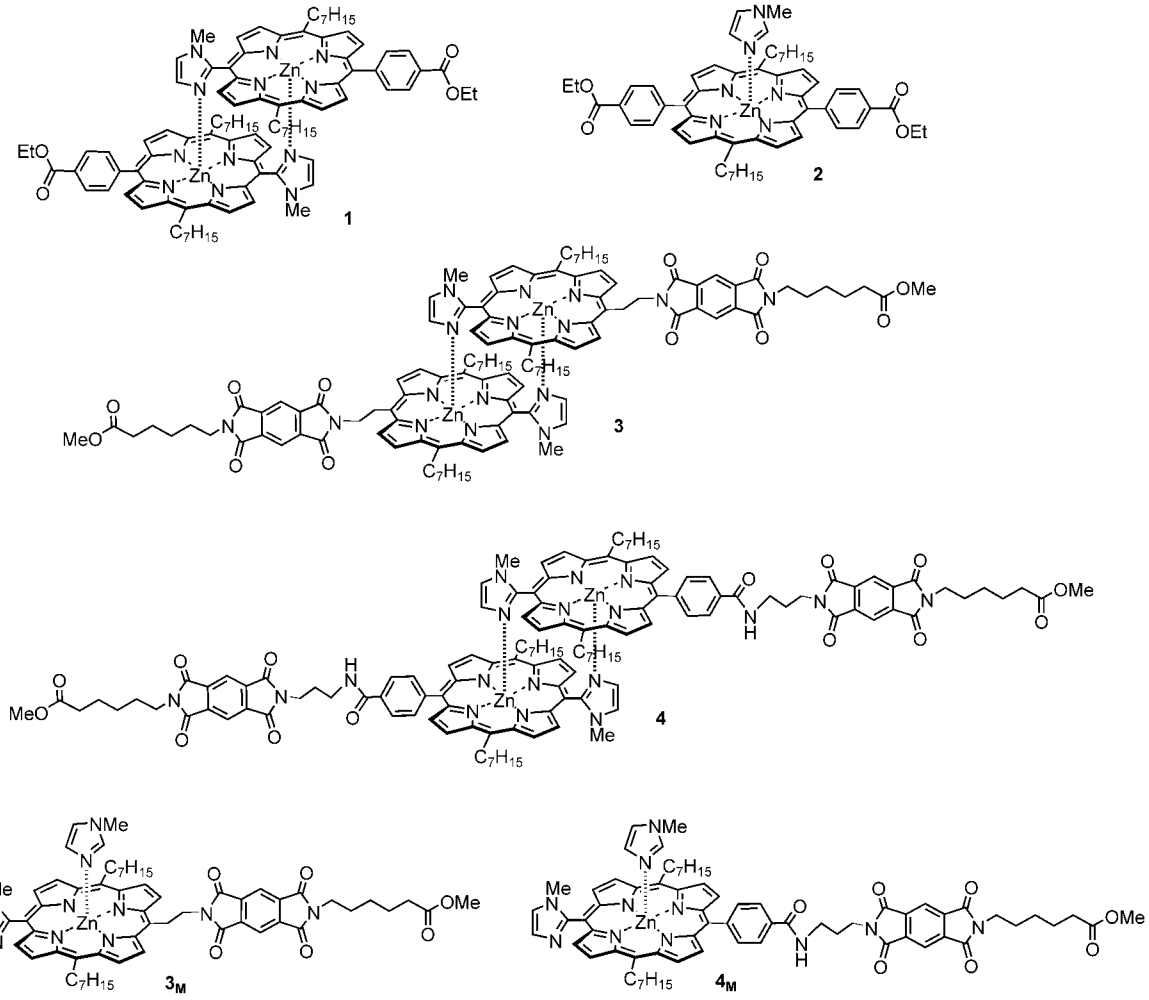

electron oxidized state of the special pair in natural systems is consistent with an unpaired electron delocalized over two chromophores.[9] However, to the best of our knowledge, the critical role of the special pair in light-induced charge separation has not yet been clarified. In this study, the slipped cofacial porphyrin dimer was attached to a PI moiety as an electron-accepting quinone model to construct a photosynthetic reaction center, and to elucidate the effect of dimer formation on the rates of light-induced charge separation and charge recombination. The crucial role of the "special pair" in the primary charge-separating event was clearly demonstrated.

Compounds **1** and **2** were prepared and used for electrochemical measurements to investigate the effect of dimerization on the properties of the porphyrin radical cation species prior to the introduction of the electron acceptor. For the photodynamic studies, pyromellitdiimides were then introduced into zinc porphyrin dimers **3** and **4** by using appropriate spacers with center-to-center separation distances of 13.3 and 18.3 Å, respectively. Due to the characteristic absorption band of the pyromellitdiimide radical anion, as well as its appropriate one-electron reduction potential,[10] pyromellitdiimide was chosen as the electron acceptor to facilitate the analysis of electron-transfer kinetics. Compounds $\mathbf{3_M}$ and $\mathbf{4_M}$, coordinated by 1-methylimidazole, were prepared as the respective monomeric reference compounds of zinc porphyrin dimers **3** and **4** for photophysical experiments.

Results and Discussion

Synthesis: The synthetic routes to target porphyrins are shown in Scheme 1. Synthesis of **3** was described in a previous report.[11] Reaction of *n*-heptyldipyrromethane with equimolar amounts of the ethyl ester of terephthalaldehydic acid, in the presence of trifluoroacetic acid (TFA) as an acid catalyst, followed by DDQ (2,3-dichloro-5,6-dicyano-*p*-benzoquinone) oxidation, resulted in crude products of free base porphyrin **5** in a 14% yield. Purification by using SiO_2 column chromatography afforded pure **5**, which was characterized by using MALDI-TOF MS and ^{1}H NMR spectroscopy. The subsequent insertion of zinc yielded the zinc porphyrin **6** almost quantitatively and was used without further purification. The solution of **2** in chloroform (1 mM), which was used for electrochemical measurements, was prepared by the addition of 12 equivalents of 1-methylimidazole. The complete association was confirmed by titration (see Experimental Section).

Porphyrin **7** was synthesized in a 7% yield by the reaction of *n*-heptyldipyrromethane with equimolar amounts of the

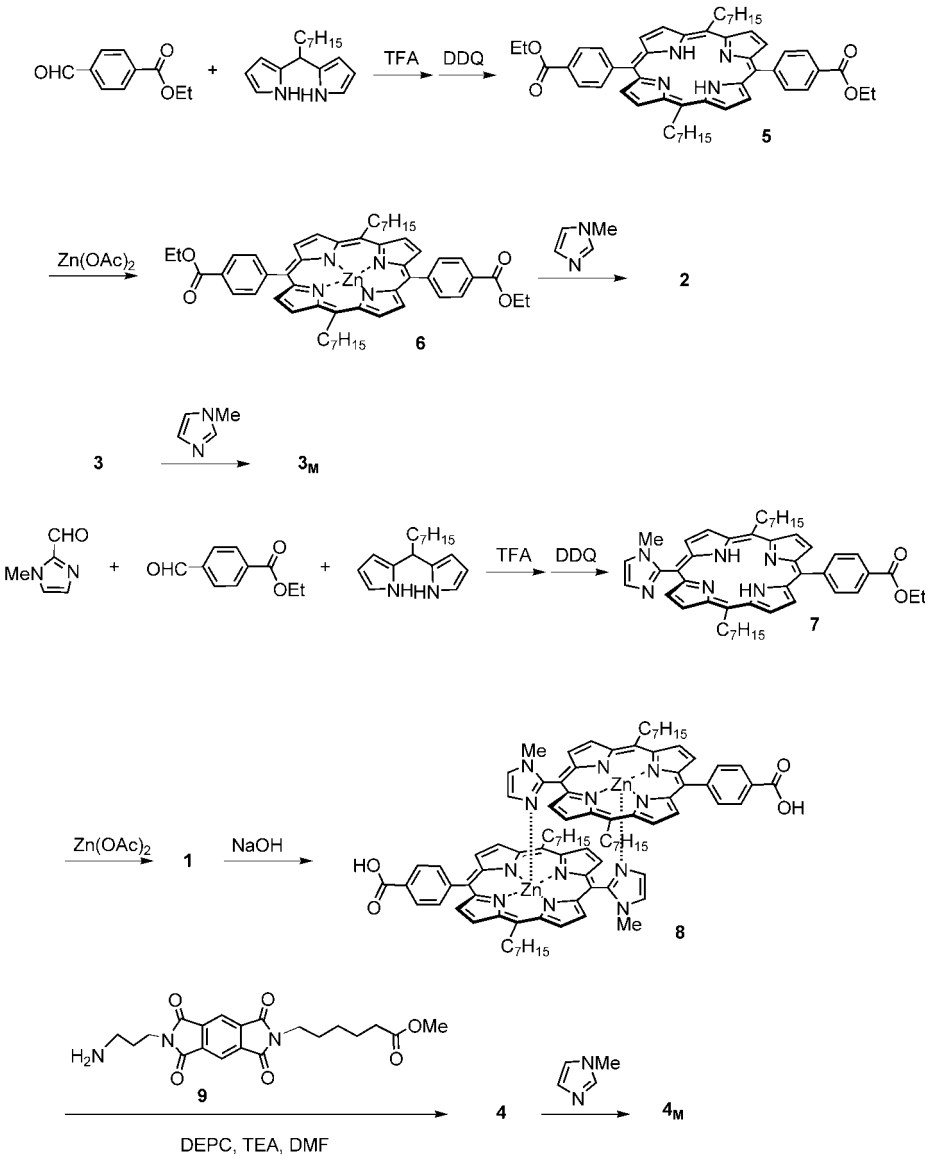

Scheme 1. Synthetic routes of porphyrin compounds. Synthesis of **3** was reported previously.[11]

ethyl ester of terephthalaldehydic acid and 1-methyl-2-formylimidazole in the presence of TFA, followed by DDQ oxidation . After purification by using SiO_2 column chromatography, the coordination dimer **1** was quantitatively obtained by the insertion of zinc. Condensation of aminopyromellitdiimide **9** and porphyrinbenzoic acid **8**, which was prepared from **1** by hydrolysis by using an activated ester with DEPC (diethylphosphorocyanidate) and triethylamine in DMF (dimethylformamide), resulted in pyromellitdiimide-substituted porphyrin **4** in an 81% yield. The solutions of $\mathbf{3_M}$ and $\mathbf{4_M}$ in chloroform, which were used for the photophysical measurements, were prepared by the addition of 220 equivalents of 1-methylimidazole (see Experimental Section).

Electrochemical study of porphyrin radical cation formation: The electrochemical properties of imidazolyl zinc porphyrins **1** and **2** were examined to elucidate the effect of dimerization on electronic coupling prior to the incorporation of an electron acceptor into the substrate. Figure 1 shows differential pulse voltammogram (DPV) charts of dimer **1** and monomer **2**. The first and second oxidation potentials of monomer **2** were observed at 381 and 756 mV, respectively. In contrast, dimer **1** revealed four, clearly separated one-electron oxidation potentials at 414, 632, 968, and 1120 mV, suggesting strong electronic interaction between the two porphyrins.[7b,8a] Notably, dimer formation did not shift the potential towards easier oxidation; rather, the second-lowest oxidation potential was shifted to a value significantly higher than the first. This was interpreted to be a consequence of delocalization of the generated radical cation over the whole π-electronic orbital of the porphyrin dimer.

The solvent dependence of the first oxidation potentials of **1** and **2** was measured in three different solvents (see Table 1). The oxidation potentials shifted to less positive values in solvents of greater polarity, indicating increased stabilization of the radical cations. The shift values for dimer **1** were approximately half of those observed for monomer **2**. The weaker solvent polarity for dimer **1** can be ascribed to the decreased charge density of the radical cation due to delocalization over the porphyrin moieties. According to the Born and

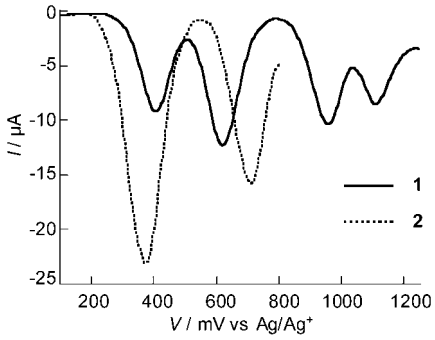

Figure 1. Differential pulse voltammograms of dimer **1** and monomer **2** in $CHCl_3$ containing 0.1 M TBAP as a supporting electrolyte with a sweep rate of 10 mV s^{-1}.

Table 1. One-electron redox potentials (mV vs Ag/Ag^+) of dimer **1** and monomer **2** measured in various solvents by using differential pulse voltammetry with a sweep rate of 10 mV s^{-1} and 0.1 M TBAP as the supporting electrolyte.

Compound	Chloroform (4.8)[a]	Dichloromethane (9.0)[a]	Acetone (21)[a]
2	381	331	305
1	414	391	378

[a] Dielectric constant.

Marcus equations, the difference in the solvent dependence of the oxidation potentials can be used to calculate the difference in the reorganization energy. The solvent dependence of the oxidation potential arising from the dielectric solvation is represented by Equation (1) in the framework of Born approximation, in which ε_s and ε_r are the dielectric constants of the solvent and reference solvent, respectively.

$$\Delta E(D/D^+) = e^2/(4\pi\varepsilon_0)(1/2R)(1/\varepsilon_s - 1/\varepsilon_r) \quad (1)$$

Plots of the oxidation potential $E(D/D^+)$, measured in various solvents, against $1/\varepsilon$ for dimer and monomer, in which the slope and y axis intercept correspond to $e^2/(4\pi\varepsilon_0 2R)$ and the oxidation potential at $\varepsilon \rightarrow \infty$, respectively, indicated the radii of radical cations to be 27 and 15 Å, respectively. Although the calculated radii are almost three times larger than the estimated values, the difference between dimer and monomer clearly exists. By applying these values to the Marcus Equation [Eq. (2)], in which ε_∞ and ε_s are the dielectric constants for the optical region and static constant, respectively, the shift of the reorganization energy was estimated to be approximately 0.1 eV.

$$\Delta\lambda s = e^2/(4\pi\varepsilon_0)[1/(2R_{dimer}) - 1/(2R_{monomer})](1/\varepsilon_\infty - 1/\varepsilon_s) \quad (2)$$

Photophysical properties of porphyrin–pyromellitdiimide dyads: The time constants of photoinduced charge separation (CS) and charge recombination (CR) for porphyrin/electron-acceptor systems were estimated from the time-resolved transient absorption spectra of dimers **3** and **4**, and the corresponding monomers $\mathbf{3_M}$ and $\mathbf{4_M}$, with excitation at the Q-band of zinc porphyrin. The reference monomers $\mathbf{3_M}$ and $\mathbf{4_M}$ were obtained by the dissociation of the complementary coordination dimer, following addition of 1-methylimidazole (44.2 mM) to the chloroform solutions of **3** and **4**, respectively. The time constants of the CS and CR reactions were obtained from fs (femtosecond) and ps (picosecond) measurements of the S_1 fluorescence decay profiles, as well as from transient absorption spectroscopy, which detected the evolution of the $S_n \leftarrow S_1$ transition and the pyromellitdiimide radical anion ($PI^{\bullet-}$).

Figure 2 shows time-resolved transient absorption spectra of **3**, $\mathbf{3_M}$, **4**, and $\mathbf{4_M}$ excited by a 15 ps fwhm (full width at half maximum) laser pulse at 532 nm. In all cases, absorptions at 465 and 730 nm were assigned to the $S_n \leftarrow S_1$ transition of zinc porphyrin and the absorption of the $PI^{\bullet-}$ radical ion, respectively. The appearance of the characteristic absorption of the $PI^{\bullet-}$ radical ion soon after excitation indicates that, in the cases of **3**, $\mathbf{3_M}$, and **4**, the CS rate constants

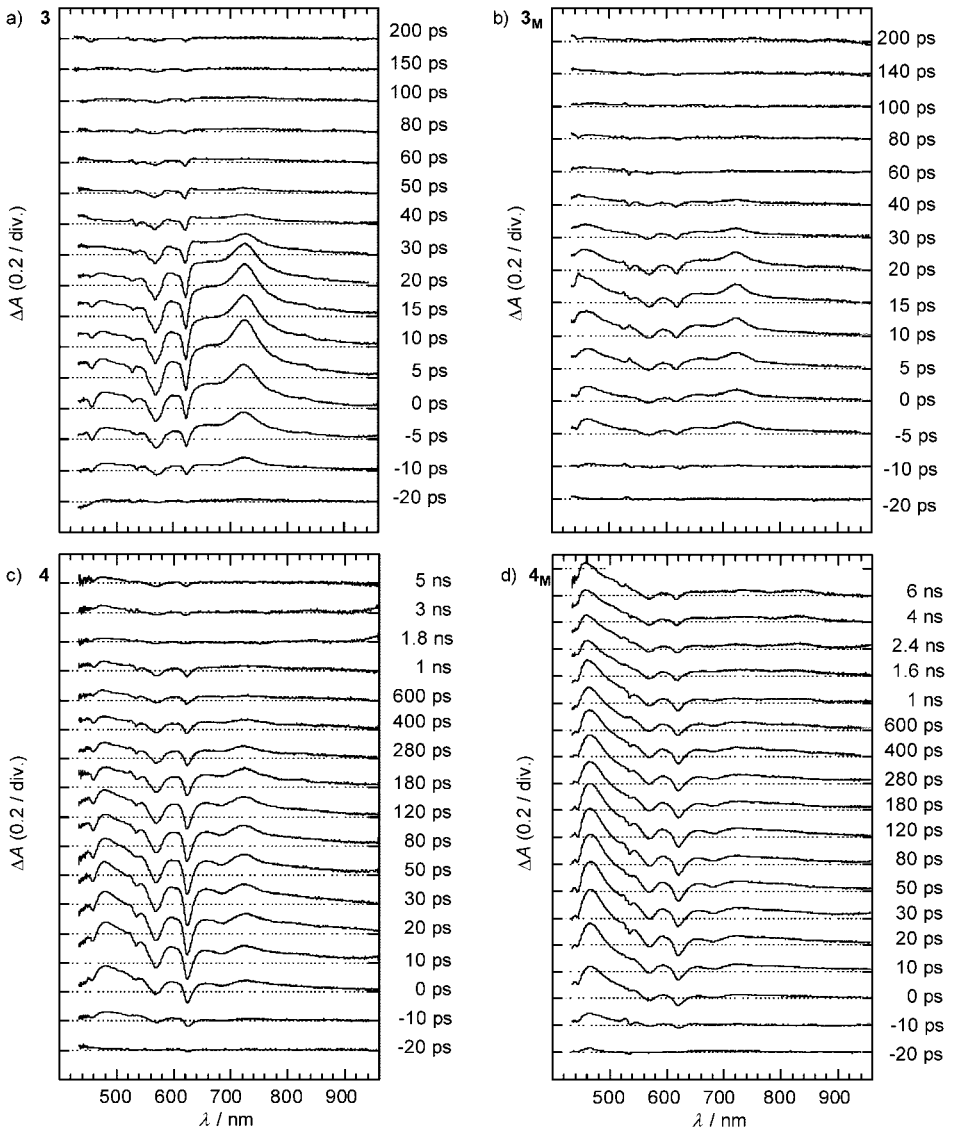

Figure 2. Time-resolved transient absorption spectra of a) **3**, b) $\mathbf{3_M}$, c) **4**, and d) $\mathbf{4_M}$ in chloroform, excited with a 15 ps fwhm laser pulse at 532 nm.

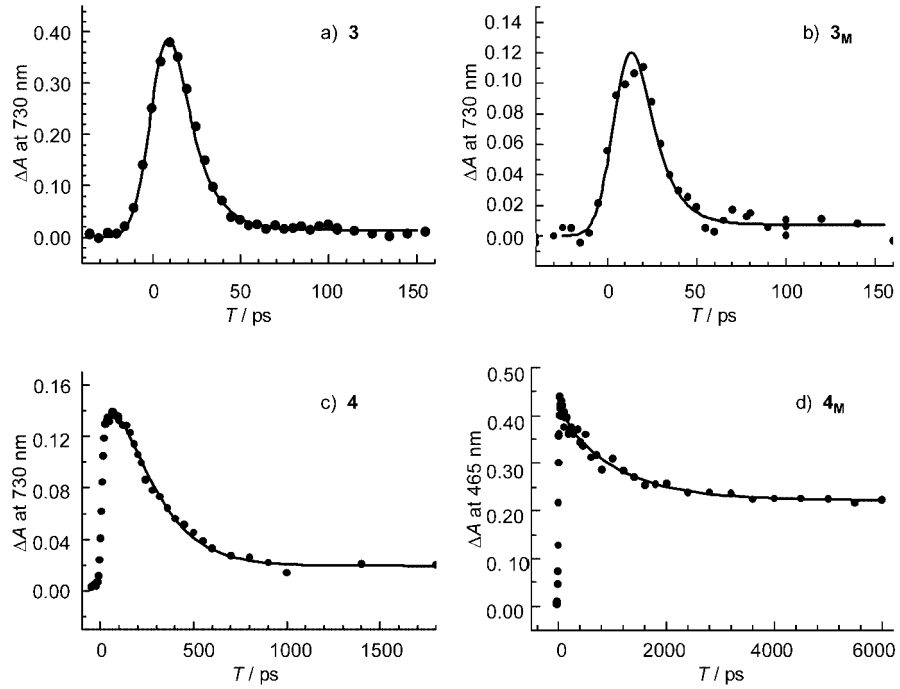

Figure 3. Time profiles of the transient absorptions at 730 nm for a) **3**, b) $\mathbf{3_M}$, and c) **4**, and at 465 nm for d) $\mathbf{4_M}$.

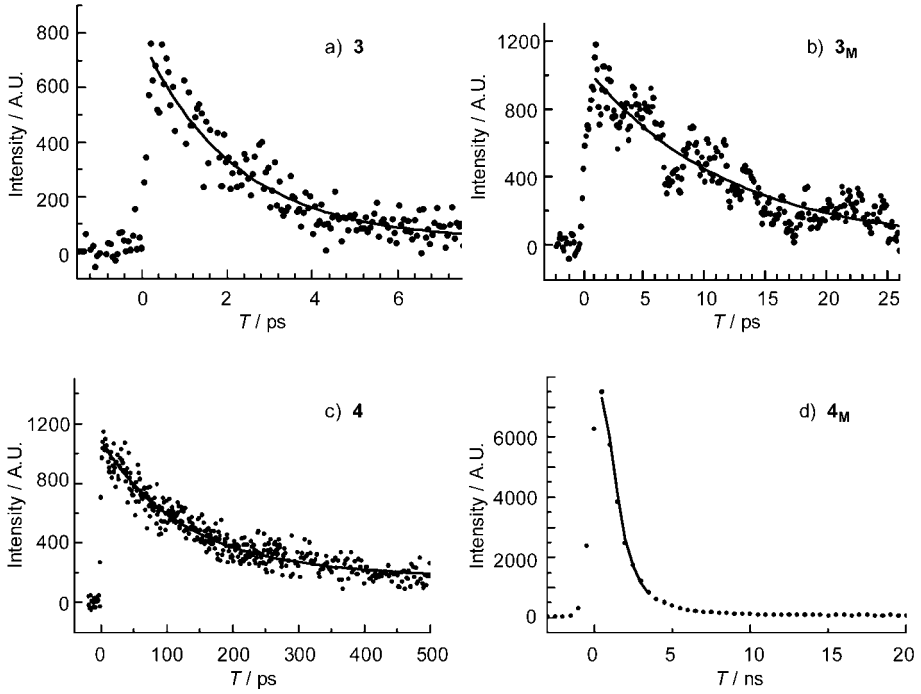

Figure 4. Fluorescence decays of a) **3**, b) $\mathbf{3_M}$, and c) **4** measured by using the femtosecond up-conversion technique, and d) $\mathbf{4_M}$ measured by using a pulsed-N_2-dye laser with a streak camera.

are large. In the transient absorption spectra of $\mathbf{4_M}$ (Figure 2d), clear absorption due to the $PI^{\bullet-}$ radical ion was not observed. The dynamic behavior of the $\mathbf{4_M}$ system is discussed below. The time profile of the transient absorption at 730 nm for dimer **3** (Figure 3a) shows the rapid appearance of the $PI^{\bullet-}$ radical ion, followed within a few tens of picoseconds by decay. The solid line in Figure 3a is the curve calculated with the rise and decay time constants of 2 ps and 12 ps, respectively, and a pulse duration of 15 ps; this plot demonstrates that the experimental results can be reproduced by using these time constants. The fluorescence lifetime of **3** was determined to be 1.7 ps by the time-resolved fluorescence measurement, shown in Figure 4a. In addition, the rise of the transient absorbance at 720 nm, following excitation with a femtosecond 550 nm laser pulse, was observed with the time constants of 1.8 ± 0.2 ps (Figure 5). These results indicate that the time constant of CS is approximately 2 ps, followed by the CR process with a time constant of 12 ps. Similarly, the time constants of CS and CR for dimer **4** were determined from the transient absorption (Figures 2c and 3c) and fluorescence lifetime measurements (Figure 4c) to be 120 and 160 ps, respectively.

Figure 6 shows the time profile of the transient absorbance of monomer $\mathbf{3_M}$ monitored at 720 nm, following excitation with a femtosecond 550 nm laser pulse. The solid line represents the results calculated from the biphasic process with the faster time constant of 3.0 ± 0.2 ps (rise) and the slower one of 9.5 ± 0.5 ps (decay). The convolution curve calculated by using these time constants and the pulse durations, which was shown as the solid line in Figure 3b, reproduced the time profile monitored at 730 nm after applying the picosecond 532 nm laser pulse. These results indicate that the appearance and disappearance time constants of the $PI^{\bullet-}$ radical ion are 3 and 10 ps, respectively. In contrast to **3**, the absorption intensity of the $PI^{\bullet-}$ radical ion at 730 nm for monomer $\mathbf{3_M}$ was less than that of the $S_n \leftarrow S_1$ transition at around 470 nm, as seen in Figure 7, in which the superimposed spectra were extracted from Figure 2a and b, respectively. The following simple kinetic analyses for the $PI^{\bullet-}$ radical ion may explain the decrease in the $PI^{\bullet-}$ radical ion absorption observed for $\mathbf{3_M}$ relative to that observed for

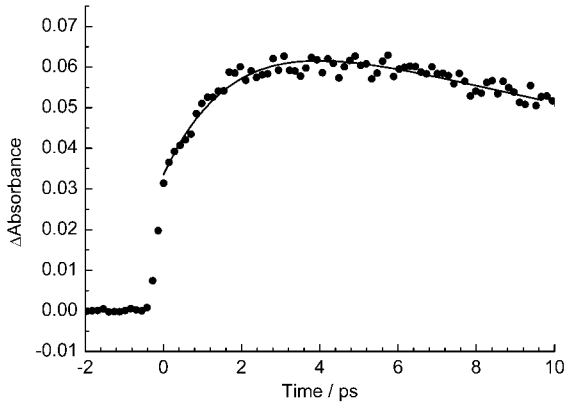

Figure 5. Time profile of transient absorbance of **3** in chloroform, monitored at 720 nm after excitation with a 550 nm femtosecond laser pulse.

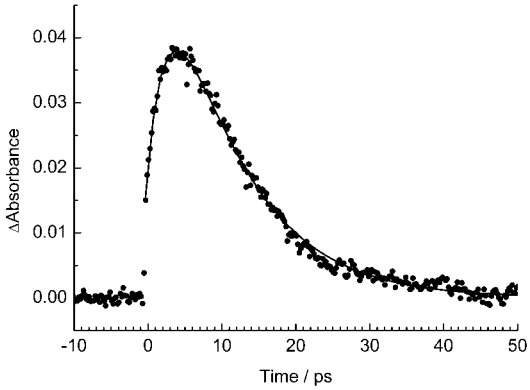

Figure 6. Time profile of transient absorbance of $\mathbf{3_M}$ in chloroform, monitored at 720 nm after excitation with a 550 nm femtosecond laser pulse.

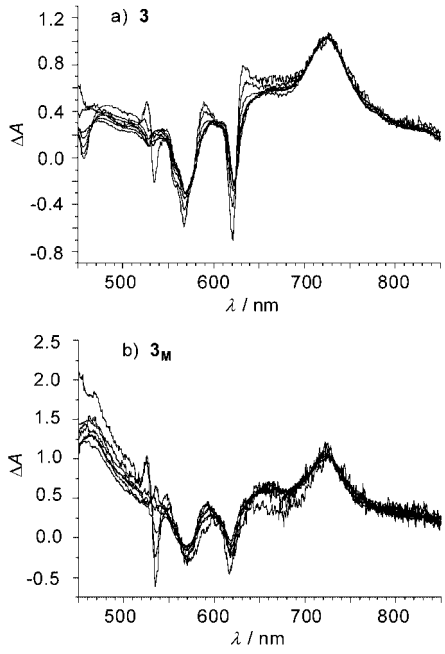

Figure 7. Superimposed transient absorption spectra of a) **3** and b) $\mathbf{3_M}$ from −5 to 40 ps. Data were extracted from Figure 2a and b, and normalized at 730 nm.

3. Because the $PI^{\bullet-}$ radical ion is produced from the porphyrin S_1 state by the CS process and disappears by the CR process, the intensity of the transient absorption of the $PI^{\bullet-}$ radical ion at time t ($A(t)_{PI}$), can be calculated by using rate constants of k_{CS} and k_{CR}, as shown in Equation (3), in which ε_{PI} is an absorption coefficient of the $PI^{\bullet-}$ radical ion, and a_0 denotes an initial concentration of the S_1 state.

$$A(t)_{PI} = [\varepsilon_{PI} a_0 k_{CS}/(k_{CS}-k_{CR})][\exp(-k_{CR}t)-\exp(-k_{CS}t)] \quad (3)$$

This equation shows that the intensity of transient absorption of the $PI^{\bullet-}$ radical ion depends on the factor of $k_{CS}/(k_{CS}-k_{CR})$. If the reciprocals of the time constants 3 and 10 ps obtained for $\mathbf{3_M}$ are assigned to k_{CS} and k_{CR}, respectively, then the relative absorption intensity of the $PI^{\bullet-}$ radical ion for the $S_n \leftarrow S_1$ absorption for $\mathbf{3_M}$ must be almost equivalent to that for **3**, since the CS and CR time constants in both cases are almost equivalent. On the other hand, if the assignment of the CS and CR time constants for $\mathbf{3_M}$ is reversed, that is, $\tau_{CS} > \tau_{CR}$, then no contradiction exists and the observation can be easily explained. To confirm the assignment of the CS process, the fluorescence lifetime was also measured. Although the S/N ratio was poor in the upconversion measurement, we could confidently estimate the lifetime to be approximately 10 ps (Figure 4b), which was similar to the time constant assigned to τ_{CS} obtained in the above analysis. From these results, it can be concluded that the components of 3 and 10 ps are assigned to CR and CS processes, respectively.

In the case of $\mathbf{4_M}$, the absorption of the $PI^{\bullet-}$ radical ion at 730 nm was very weak. Therefore, the time profile of transient absorption at 465 nm was analyzed, as shown in Figure 3d. The time constant was detected as a single component of 1 ns. This value was in agreement with the component of 920 ± 100 ps from the fluorescence lifetime measurement, as shown in Figure 4d [the fluorescence lifetimes of $\mathbf{4_M}$ and **2** (not shown) were determined to be 920 ± 100 ps and 2.4 ± 0.1 ns, respectively]. Furthermore, the fluorescence emission of $\mathbf{4_M}$ was remarkably quenched, relative to that of **2**; it exhibited a quenching efficiency of 70.3% (Table 2) due to electron transfer. Therefore, the decay with a time constant of 1 ns was assigned to CS. The rate of the CR process was estimated to be much faster than that of the CS process (probably shorter than 100 ps), because the absorp-

Table 2. Kinetic parameters of dimers **3**, **4** and corresponding monomers $\mathbf{3_M}$, $\mathbf{4_M}$ in $CHCl_3$.

Compound	τ_{CS} [ps][a]	f_{CS}[b]	τ_{CR} [ps][a]	f_{CR}[b]	τ_f [ps][c]	Q_{eff} [%][d]
$\mathbf{3_M}$	10		3		10	99.1
3	2	2.5	12	4.0	2	99.5
$\mathbf{4_M}$	1000		< 100		920	70.3
4	120	4.0	160	1.6	120	94.6

[a] Time constants obtained by measuring time-resolved transient absorption. [b] Dimer effects for the acceleration and deceleration (see main text). [c] Fluorescence lifetime. [d] Quenching efficiencies defined as $Q_{eff} = (1 - I_{compound}/I_{reference}) \times 100$, in which I is fluorescence intensity. The reference compounds for dimer and monomer were **1** and **2**, respectively.

tion of the PI anion at 730 nm was very weak, as indicated in Equation (3).

These results are summarized in Table 2. Comparison of the time constants of dimers **3** and **4** with those of the corresponding monomers clearly indicates that, in the photoinduced electron-transfer reactions, dimer formation accelerates the CS rate, whereas it decelerates the CR rate. The dimer effect for the acceleration of the CS rate and the deceleration of the CR rate, defined by $f_{CS}=\tau_{CS,monomer}/\tau_{CS,dimer}/2$ and $f_{CR}=\tau_{CR,monomer}/\tau_{CR,dimer}$, respectively, is also listed in Table 2. In the case of CS, the presence of two electron acceptors in the dimer molecule was considered as a concentration factor of two. On the other hand, the CR rate of the dimer could not be affected by the presence of another neutral PI group, because the ion pair of the porphyrin cation and the PI anion in the charge-separated state is independent of the neutral PI. These f_{CS} and f_{CR} values clearly demonstrate the dimer effect for the favorable charge separation. The fluorescence quenching efficiencies, Q_{eff}, of the dimers and monomers in $CHCl_3$ were obtained by comparing fluorescence intensities with those of reference compounds **1** and **2** (Table 2). The efficiencies for dimers **3** and **4** were significantly higher than those of the corresponding monomers $\mathbf{3_M}$ and $\mathbf{4_M}$. The trend is the same as that seen for the order of the CS rates and indicates efficient electron transfer for the dimers.

The electrochemical studies revealed that the energy levels of the charge-separated state for monomers $\mathbf{3_M}$, $\mathbf{4_M}$ and dimers **3**, **4** were 1.21, 1.31 and 1.25, 1.34 eV, respectively (as shown in the Supporting Information for this paper). Dimers **3** and **4** had slightly higher potentials than the corresponding monomers $\mathbf{3_M}$ and $\mathbf{4_M}$. However, the small shift to higher energy levels for the dimers does not explain the acceleration of the CS rate and deceleration of the CR rate that were observed experimentally.[12] We propose that this may be explained by the change in reorganization energy upon dimer formation. As outlined above, the radical cation is delocalized over two porphyrin π orbitals; this spread causes a decrease in the charge density of the dimer. Therefore, the dimer may have a smaller environmental reorganization energy (λ_D) than the corresponding monomer (λ_M). According to the Marcus theory,[12] the Marcus parabola of the dimer is expected to shift towards the left as the reorganization energy (λ) decreases, as illustrated in Figure 8. Therefore, the small reorganization energy may cause an increase in the CS rate from the normal region to the top region, and a decrease in the CR rate into the lower inverted region. Consequently, the forward electron transfer was accelerated, whereas the reverse electron transfer was decelerated. This interpretation, elucidated from the photophysical dynamics, is in agreement with the electrochemical study of the decrease in the reorganization energy from monomer to dimer.

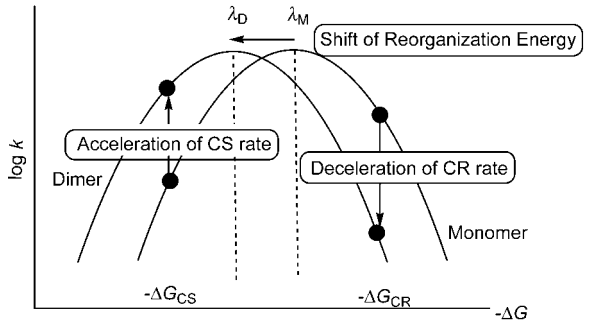

Figure 8. Marcus parabolas of monomer and dimer, in which the delocalization of the radical cation over dimer porphyrins is considered to be an explanation for the CS and CR rates. The terms k and $-\Delta G$ represent the rate constant and free energy gap, respectively.

Conclusion

The slipped cofacial dimer delocalizes the radical cation, generated in the photoinduced redox reaction, over two porphyrin units, and accelerates the CS rate, while decelerating the CR rate. The advantage of the charge separation reaction for the dimer could be attributed to a smaller reorganization energy. These results, from a simple model system comparing dimers and monomers, demonstrate the important role of the special-pair arrangement in the charge-separating event in bacterial photosynthesis. The special-pair arrangement in the same bacteriochlorophylls may be beneficial for charge separation by delocalizing the radical cation generated by the redox reaction. This study provides an insight into the facilitated electron transfer of an artificial special pair; these results will be helpful not only for our understanding of natural photosynthetic systems, but also for the design of artificial ones.

Experimental Section

Synthesis of **3** was described in a previous report.[11]

Synthesis of 5,15-bis(*n*-heptyl)-10-(1-methylimidazole-2-yl)-20-(4-ethoxycarbonylphenyl)porphine (7): Under an argon atmosphere, 1-methylimidazole-2-carboxyaldehyde (2.05 mmol), the ethyl ester of terephthalaldehydic acid (2.05 mmol), and *meso*-(*n*-heptyl)dipyrromethane (4.10 mmol) were dissolved in chloroform (410 mL), and TFA (4.10 mmol) was added. After stirring for 6 h at room temperature, DDQ (6.15 mmol) was added, and the reaction mixture was stirred for a further 1 h. The reaction solution was washed with aqueous sodium bicarbonate and water, and the organic layer was evaporated. The residue was purified by using silica gel column chromatography (eluent: chloroform/methanol = 20:1) to yield 0.143 mmol (6.98 %) of **7**. ^{1}H NMR (270 MHz, $CDCl_3$, TMS): $\delta=9.46$ (d, $J=4.86$ Hz, 2H; pyrrole βH), 9.41 (d, $J=4.86$ Hz, 2H; pyrrole βH), 8.81 (d, $J=3.24$ Hz, 2H; pyrrole βH), 8.78 (d, $J=3.24$ Hz, 2H; pyrrole βH), 8.44 (d, $J=7.83$ Hz, 1H; phenyl-H), 8.41 (d, $J=7.83$ Hz, 1H; phenyl-H), 8.33 (d, $J=7.83$ Hz, 1H; phenyl-H), 8.20 (d, $J=7.83$ Hz, 1H; phenyl-H), 7.68 (s, 1H; imidazole-H), 7.48 (s, 1H, imidazole-H), 4.95 (m, 4H; αCH_2), 4.60 (q, $J=7.29$ Hz, 2H; CO_2CH_2), 3.41 (s, 3H; NCH_3), 2.50 (m, 4H, βCH_2), 1.32 (t, $J=7.29$ Hz, 3H; CO_2CH_2–CH_3), 0.88 (t, $J=7.29$ Hz, 6H; alkyl CH_3), −2.67 ppm (d, 2H; pyrrole-NH); UV/Vis ($CHCl_3$): $\lambda_{max}=418$, 517, 552, 593, 649 nm; fluorescence ($CHCl_3$): $\lambda_{max}=656$, 723 nm; MS (MALDI-TOF): m/z: 735.42 $[M+H]^+$ (calcd: 735.43).

Synthesis of 5,15-bis(*n*-heptyl)-10-(1-methylimidazole-2-yl)-20-(4-ethoxycarbonylphenyl)porphinatozinc(II) (1): A saturated solution of zinc acetate dihydrate in methanol (0.6 mL) was added to a solution of free base porphyrin **7** (18.9 μmol) in chloroform (2 mL). After stirring for 3 h at room temperature, the solution was washed with water, and the organic layer was evaporated to yield 18.7 μmol (98.7 %) of **1**. UV/Vis ($CHCl_3$): $\lambda_{max}=414$, 438, 565, 622 nm; fluorescence ($CHCl_3$): $\lambda_{max}=627$, 684 nm; MS (MALDI-TOF): m/z: 797.43 $[M+H]^+$ (calcd: 797.43).

Synthesis of 5,15-bis(heptyl)-10-(1-methylimidazole-2-yl)-20-(4-carboxylphenyl)porphinatozinc(II) (8): A solution of NaOH (0.5 mL, 8 N) was added to a solution of **1** (18.7 μmol) in methanol/THF (1:2, 2.1 mL). After stirring for 2 h at room temperature, the reaction solution was evaporated. The residue was acidified to pH 4 by adding aqueous 1 N HCl solution, and extracted with $CHCl_3$. The organic layer was washed with water. The solvent was removed by evaporation to yield 17.0 μmol (90.9 %) of **8**. ^{1}H NMR (270 MHz, $CDCl_3$, TMS): $\delta = 9.59$ (d, $J = 4.86$ Hz, 2H; pyrrole βH), 9.00 (d, $J = 3.24$ Hz, 2H; pyrrole βH), 8.91 (d, $J = 4.86$ Hz, 2H; pyrrole βH), 8.78 (d, $J = 7.83$ Hz, 1H; phenyl-H), 8.63 (d, $J = 7.83$ Hz, 1H; phenyl-H), 8.47 (d, $J = 7.83$ Hz, 1H; phenyl-H), 8.24 (d, $J = 7.83$ Hz, 1H; phenyl-H), 5.56 (s, 1H; imidazole-H), 5.43 (d, $J = 3.24$ Hz, 2H; pyrrole βH), 4.28 (m, 4H; αCH_2), 2.94 (m, 4H; βCH_2), 2.13 (s, 1H; imidazole-H), 2.05 (m, 4H; γCH_2), 1.69 (s, 3H; NCH_3), 1.01 ppm (t, $J = 7.29$ Hz, 6H; alkyl CH_3); UV/Vis ($CHCl_3$): $\lambda_{max} = 414$, 438, 565, 622 nm; fluorescence ($CHCl_3$): $\lambda_{max} = 628$, 685 nm; MS (MALDI-TOF): m/z: 769.91 $[M+H]^+$ (calcd: 769.92).

Synthesis of 5,15-bis(*n*-heptyl)-10,20-bis(4-ethoxycarbonylphenyl)porphine (5): Under an argon atmosphere, the ethyl ester of terephthalaldehydic acid (4.10 mmol), and *meso*-(*n*-heptyl)dipyrromethane (4.10 mmol) were dissolved in chloroform (410 mL), and then TFA (4.10 mmol) was added. After stirring for 6 h at room temperature, DDQ (6.15 mmol) was added, and the reaction mixture was stirred for a further 1 h. The reaction solution was washed with aqueous sodium bicarbonate, and the organic layer was evaporated. The residue was purified by using silica gel column chromatography (eluent: chloroform/methanol = 20:1) to yield 0.293 mmol (14.3 %) of **5**. ^{1}H NMR (270 MHz, $CDCl_3$, TMS): $\delta = 9.43$ (d, $J = 3.24$ Hz, 4H; pyrrole βH), 8.80 (d, $J = 3.24$ Hz, 4H; pyrrole βH), 8.44 (d, $J = 7.83$ Hz, 4H; phenyl-H), 8.28 (d, $J = 7.83$ Hz, 1H; phenyl-H), 4.95 (m, 4H; αCH_2), 4.60 (q, $J = 7.29$ Hz, 4H; CO_2CH_2), 2.50 (m, 4H; βCH_2), 1.32 (t, $J = 7.29$ Hz, 6H; CO_2CH_2-CH_3), 0.88 (t, $J = 7.29$ Hz, 6H; alkyl CH_3), −2.69 ppm (s, 2H; pyrrole-NH); UV/Vis ($CHCl_3$): $\lambda_{max} = 418$, 517, 552, 593, 649 nm; fluorescence ($CHCl_3$): $\lambda_{max} = 656$, 723 nm; MS (MALDI-TOF): m/z: 803.44 $[M+H]^+$ (calcd: 803.45).

Synthesis of 5,15-bis(*n*-heptyl)-10,20-bis(4-ethoxycarbonylphenyl)porphinatozinc(II) (6): A saturated solution of zinc acetate dihydrate in methanol (0.6 mL) was added to a solution of free-base porphyrin **5** (20.3 μmol) in chloroform (2 mL). After stirring for 3 h at room temperature, the solution was washed with water, and the organic layer was evaporated to yield 19.5 μmol (96.1 %) of **6**. ^{1}H NMR (270 MHz, $CDCl_3$, TMS): $\delta = 9.54$ (d, $J = 3.24$ Hz, 4H; pyrrole βH), 8.89 (d, $J = 3.24$ Hz, 4H; pyrrole βH), 8.45 (d, $J = 7.83$ Hz, 4H; phenyl-H), 8.28 (d, $J = 7.83$ Hz, 1H; phenyl-H), 4.99 (m, 4H; αCH_2), 4.58 (q, $J = 7.29$ Hz, 4H; CO_2CH_2), 2.55 (m, 4H; βCH_2), 1.32 (t, $J = 7.29$ Hz, 6H; CO_2CH_2-CH_3), 0.88 ppm (t, $J = 7.29$ Hz, 6H; alkyl CH_3); UV/Vis ($CHCl_3$): $\lambda_{max} = 414$, 438, 565, 622 nm; fluorescence ($CHCl_3$): $\lambda_{max} = 627$, 684 nm; MS (MALDI-TOF): m/z: 809.31 $[M+H]^+$ (calcd: 809.30).

Preparation of zinc porphyrin monomer coordinated by 1-methylimidazole (2): To determine the equivalent of 1-methylimidazole for monomer formation, zinc porphyrin **6** (0.220 μmol) and tetra-*n*-butylammonium perchlorate (TBAP, 0.03 mmol, 0.1 M) were dissolved in chloroform (0.3 mL), and 1-methylimidazole was titrated into this solution (from 1 to 12 equiv), by UV/Vis spectroscopy. During the titration of 1-methylimidazole, the Q-band at 565 nm was shifted to 581 nm, and the intensity of absorption at 581 nm was saturated at the addition of 11 equiv of 1-methylimidazole. Therefore, a solution of zinc porphyrin monomer **2**, coordinated by 1-methylimidazole, was prepared for the DPV measurement by dissolving zinc porphyrin monomer **6** (2 μmol), TBAP (0.2 mmol, 0.1 M), and 1-methylimidazole (12 equiv) in chloroform (2 mL).

Synthesis of imidazolyl zinc porphyrin dimer attached by pyromellitdiimide (4): Under an argon atmosphere, **8** (7.76 μmol), **9** (59.9 μmol), and diethyl phosphorocyanidate (DEPC, 27.5 μmol) were dissolved in DMF (1.2 mL), and then triethylamine (59.9 μmol) was added at 0 °C. After stirring for 5 h at 0 °C and for a further 12 h at room temperature, the reaction solution was evaporated. The residue was purified by using silica gel column chromatography (eluent: chloroform/acetone = 10:1) to yield 6.17 μmol (81.2 %) of **4**. ^{1}H NMR (270 MHz, $CDCl_3$, TMS): $\delta = 9.57$ (d, $J = 4.82$ Hz, 2H; pyrrole βH), 9.00 (d, $J = 3.26$ Hz, 2H; pyrrole βH), 8.93 (d, $J = 4.82$ Hz, 2H; pyrrole βH), 8.75 (d, $J = 7.83$ Hz, 1H; phenyl-H), 8.42 (d, $J = 7.83$ Hz, 1H; phenyl-H), 8.40 (d, $J = 7.83$ Hz, 1H; phenyl-H), 8.27 (d, $J = 7.83$ Hz, 1H; phenyl-H), 7.42 (s, 2H; imide, phenyl-H), 7.15 (s, 1H; amide-NH), 5.56 (s, 1H; imidazole-H), 5.46 (d, $J = 3.26$ Hz, 2H; pyrrole βH), 5.07 (m, 4H; αCH_2), 3.65 (s, 3H; CO_2CH_3), 2.92 (m, 4H; βCH_2), 2.28 (s, 1H; imidazole-H), 2.07 (m, 4H; γCH_2), 1.87 (s, 3H; imidazole-NCH_3), 1.06 ppm (t, $J = 7.29$ Hz, 6H; alkyl CH_3); UV/Vis ($CHCl_3$): $\lambda_{max} = 414$, 438, 565, 622 nm; fluorescence ($CHCl_3$): $\lambda_{max} = 626$, 685 nm; MS (MALDI-TOF): m/z: 809.31 $[M+H]^+$ (calcd: 809.30).

Preparations of 3_M and 4_M for photophysical measurements: Zinc porphyrin dimer **3** or **4** (0.24 μmol) was dissolved in chloroform (1.2 mL) and 1-methylimidazole (53.0 μmol) was added. Following the addition of 1-methylimidazole, the split Soret bands at 414 and 438 nm, which were typically observed in the complementary dimer,[6] became single peaks at 420 nm, indicating the dissociation of dimer into monomer.

Measurements and analyses of photoinduced electron-transfer dynamics: To examine the photodynamics of dimers **3** and **4**, and monomers $\mathbf{3_M}$ and $\mathbf{4_M}$, transient absorption spectra were measured by using femtosecond (560 nm, 150 fs) and picosecond (532 nm, 15 ps) laser pulses. To analyze the electron-transfer dynamics, the absorption of the one-electron-reduced form of the electron acceptor ($PI^{\bullet-}$) at 730 nm was monitored.[10] The fluorescence lifetime was determined by using the femtosecond up-conversion technique to confirm the CS time constant for **3**, $\mathbf{3_M}$, and **4**. The gate pulse and the excitation wavelengths were 820 and 410 nm, respectively, with pulse duration of ~100 fs. In the case of $\mathbf{4_M}$, the fluorescence lifetime was measured with an 800 ps-pulse-N_2-dye laser excited at 400 nm and detected at 620 nm with a streak camera.

Acknowledgments

This work was supported by CREST (Japan Science and Technology Corporation), and by Grant-in-Aids for Scientific Research (A) (No. 15205020), for Scientific Research on Priority Areas (No. 15036248, Reaction Control of Dynamic Complexes), and for Scientific Research on Priority Areas (417, No.15033242) from the Ministry of Education, Culture, Sports, Science and Technology, Japan (Monbu Kagakusho).

[1] a) *The Photosynthetic Reaction Center, Vols. I and II* (Eds.: J. Deisenhofer, J. R. Norris), Academic Press, New York, **1993**; b) *The Reaction Center of Photosynthetic Bacteria* (Ed.: M. E. Michel-Beyerle), Springer, Berlin/Heidelberg, **1996**.

[2] a) J. Deisenhofer, O. Epp, K. Miki, R. Huber, H. Michel, *Nature* **1985**, *318*, 618; b) J. Deisenhofer, H. Michel, *Science* **1989**, *245*, 1463; c) P. Allen, G. Feher, T. O. Yeates, D. C. Rees, J. Deisenhofer, H. Michel, R. Huber, *Proc. Natl. Acad. Sci. USA* **1986**, *83*, 8589; d) J. Deisenhofer, O. Epp, I. Sinning, H. Michel, *J. Mol. Biol.* **1995**, *246*, 429; e) P. Jordan, P. Fromme, H.-T. Witt, O. Klukas, W. Saenger, N. Krauss, *Nature* **2001**, *411*, 909.

[3] a) D. Gust, T. A. Moore, A. L. Moore, *Acc. Chem. Res.* **2001**, *34*, 40; b) H. Imahori, Y. Sakata, *Eur. J. Org. Chem.* **1999**, 2445.

[4] a) M. A. Wasielewski, *Chem. Rev.* **1992**, *92*, 435; b) D. Gust, T. A. Moore in *The Porphyrin Handbook, Vol. 8* (Eds.: K. M. Kadish, K. M. Smith, R. Guilard), Academic Press, New York, **2000**, pp. 153–190; c) P. D. Harvey in *The Porphyrin Handbook, Vol. 18* (Eds.: K. M. Kadish, K. M. Smith, R. Guilard), Academic Press, New York, **2003**, pp. 63–250.

[5] a) A. Osuka, S. Nakajima, K. Maruyama, N. Mataga, T. Asahi, I. Yamazaki, Y. Nishimura, T. Ohno, K. Nozaki, *J. Am. Chem. Soc.* **1993**, *115*, 4577; b) S. Nakashima, S. Taniguchi, T. Okada, A. Osuka, Y. Mizutani, T. Kitagawa, *J. Phys. Chem. A* **1999**, *103*, 9184.

[6] a) Y. Kobuke, H. Miyaji, *J. Am. Chem. Soc.* **1994**, *116*, 4111; b) Y. Kobuke, H. Miyaji, *Bull. Chem. Soc. Jpn.* **1996**, *69*, 3563; c) Y. Kobuke, K. Ogawa, *Bull. Chem. Soc. Jpn.* **2003**, *76*, 689.

[7] a) R. T. Stibrany, J. Vasudevan, S. Knapp, J. A. Potenza, T. Emge, H. J. Schugar, *J. Am. Chem. Soc.* **1996**, *118*, 3980; b) J. Vasudevan, R. T. Stibrany, J. Bumby, S. Knapp, J. A. Potenza, T. J. Emge, H. J. Schugar, *J. Am. Chem. Soc.* **1996**, *118*, 11676.

[8] a) K. Funatsu, T. Imamura, A. Ichimura, Y. Sasaki, *Inorg. Chem.* **1998**, *37*, 4986; b) T. Imamura, K. Funatsu, S. Ye, Y. Morioka, K. Uosaki, Y. Sasaki, *J. Am. Chem. Soc.* **2000**, *122*, 9032.

[9] a) J. R. Reimers, M. C. Hutter, J. M. Hughes, N. S. Hush, *Int. J. Quantum Chem.* **2000**, *80*, 1224; b) T. Noguchi, T. Tomo, Y. Inoue, *Biochemistry* **1998**, *37*, 13614; c) S. E. J. Rigby, J. H. A. Nugent, P. J. O'Malley, *Biochemistry* **1994**, *33*, 10043.
[10] a) G. P. Wiederrecht, M. P. Niemczyk, W. A. Svec, M. R. Wasielewski, *J. Am. Chem. Soc.* **1996**, *118*, 81; b) J. A. Cowan, J. K. M. Sanders, *J. Chem. Soc. Perkin Trans. 1* **1985**, 2435.
[11] A. Nomoto, H. Mitsuoka, H. Ozeki, Y. Kobuke, *Chem. Commun.* **2003**, 1074.
[12] a) R. A. Marcus, *Can. J. Chem.* **1959**, *37*, 155; b) R. A. Marcus, *J. Chem. Phys.* **1965**, *43*, 679; c) D. Rehm, A. Weller, *Ber. Bunsenges. Phys. Chem.* **1969**, *73*, 834; d) A. Weller, *Z. Phys. Chem.* **1982**, *133*, 93; e) J. A. Schmidt, J. Y. Liu, J. R. Bolton, M. D. Archer, V. P. Y. Gadzekpo, *J. Chem. Soc. Faraday Trans. 1* **1989**, *85*, 1027.

Received: June 22, 2004
Published online: November 5, 2004

